Molecular Therapy
Nucleic Acids
Original Article

VPS33B modulates c-Myc/p53/miR-192-3p to target CCNB1 suppressing the growth of non-small cell lung cancer

Jiahao Liu,[1,6] Yinghao Wen,[1,6] Zhen Liu,[1,2,6] Shu Liu,[3,6] Ping Xu,[1] Yan Xu,[1] Shuting Deng,[1] Shulu Hu,[1] Rongcheng Luo,[1] Jingwen Jiang,[1,4] and Guifang Yu[1,5]

[1]Cancer Center, Integrated Hospital of Traditional Chinese Medicine, Southern Medical University, Guangzhou, Guangdong, P.R. China; [2]Key Laboratory of Protein Modification and Degradation, Basic School of Guangzhou Medical University, Guangzhou, Guangdong, P.R. China; [3]Department of Breast Surgery, The Affiliated Hospital of Guizhou Medical University, Guiyang, Guizhou, P.R. China; [4]Oncology Department, Hainan Province Hospital of Traditional Chinese Medicine, Haikou, Hainan, P.R. China; [5]Oncology Department, The Fifth Affiliated Hospital of Guangzhou Medical University, Guangzhou, Guangdong, P.R. China

VPS33B is reported to be a tumor suppressor in hepatocellular carcinoma, nasopharyngeal carcinoma, colon cancer, and lung adenocarcinoma. Here, we observed that reduced VPS33B protein level was an unfavorable factor that promoted the pathogenesis of non-small cell lung cancer (NSCLC) in clinical specimens. We achieved lentivirus-mediated stable overexpression of VPS33B in NSCLC cells. Increased VPS33B reduced cell cycle transition and cell proliferation of NSCLC cells *in vivo* and *in vitro*. Knocking down VPS33B restored cell growth. Mechanism analysis indicated that miR-192-3p was induced by VPS33B and acted as a tumor suppressor of cell growth in NSCLC. Further, c-Myc or p53 was identified as a transcription factor that bound to the miR-192-3p promoter and regulated its expression. miR-192-3p directly targeted cell cycle-promoted factor CCNB1 and suppressed NSCLC cell growth. VPS33B modulated c-Myc/p53/miR-192-3p signaling to target CCNB1 by reducing activation of the Ras/ERK pathway. Our study reveals a novel molecular basis for VPS33B as a tumor suppressor to participate in the pathogenesis of NSCLC.

INTRODUCTION

Lung cancer occurs when abnormal cells divide in an uncontrolled way to form a tumor in the lung. Lung cancer is one of the most common cancers in the world, including in China. The two main types of lung cancer are small cell lung cancer (SCLC) and non-small cell lung cancer (NSCLC). NSCLC mainly includes squamous cell carcinoma and adenocarcinoma and is any type of epithelial lung cancer other than SCLC. NSCLC accounts for about 85%–90% of all lung cancers.[1]

The dysfunction of a large number of genes participates in the pathogenesis of NSCLC.[2–11] VPS33B is a member of the Sec-1 domain family that may have a significant effect on vesicle-mediated protein trafficking to lysosomal compartments and in membrane docking/fusion reactions of late endosomes/lysosomes.[12] Loss of VPS33B successfully induced hepatocarcinogenesis by interacting with Sec22b and flotillin-1 in a VPS33B knockout mouse model, suggesting that VPS33B acts as a tumor suppressor in hepatocellular carcinoma (HCC).[13] We observed that VPS33B suppresses the pathogenesis of nasopharyngeal carcinoma (NPC) and colon cancer by interacting with NESG1 to modulate the feedback loop of EGFR/phosphatidylinositol 3-kinase (PI3K)/AKT/c-Myc/p53/miR-133a and EGFR/Ras/ERK/c-Myc/p53/miR-133a.[14,15] For lung adenocarcinoma (LUAD), VPS33B was found to suppress cell metastasis and chemoresistance to cisplatin in LUAD cells via inactivating EGFR/Ras/ERK-mediated EMT signals.[16] These results further support the hypothesis that VPS33B possesses tumor-suppressive characteristics. However, its function and molecular mechanism in NSCLC had not been reported.

We observed that the absence of VPS33B protein expression was an unfavorable factor that promoted NSCLC pathogenesis. Furthermore, we observed that VPS33B suppressed Ras/ERK signaling and thus regulated c-Myc/p53/miR-192-3p signaling to target the cell cycle modulator cyclin B1 (CCNB1), which reduced the cell cycle transition and cell growth in NSCLC. Our study found that VPS33B acted as a tumor suppressor to halt NSCLC pathogenesis by modulating c-Myc/p53/miR-192-3p to target CCNB1 in NSCLC.

Received 13 July 2020; accepted 10 November 2020;
https://doi.org/10.1016/j.omtn.2020.11.010.

[6]These authors contributed equally

Correspondence: Guifang Yu, Cancer Center, Integrated Hospital of Traditional Chinese Medicine, Southern Medical University, Guangzhou, Guangdong, P.R. China.
E-mail: 526136010@qq.com
Correspondence: Jingwen Jiang, Cancer Center, Integrated Hospital of Traditional Chinese Medicine, Southern Medical University, Guangzhou, Guangdong, P.R. China.
E-mail: 18673106015@163.com
Correspondence: Rongcheng Luo, Cancer Center, Integrated Hospital of Traditional Chinese Medicine, Southern Medical University, Guangzhou, Guangdong, P.R. China.
E-mail: luorc01@163.com

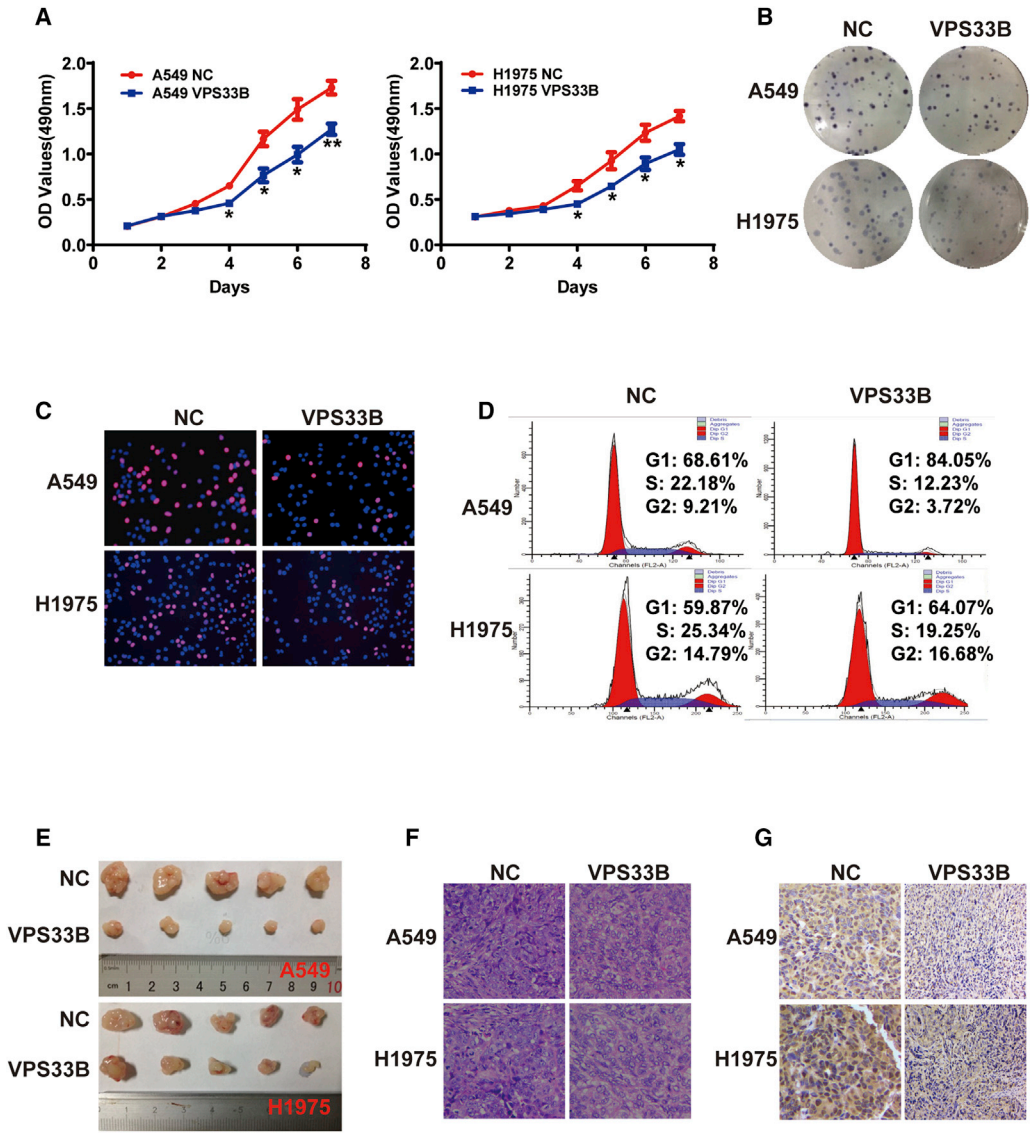

Figure 1. VPS33B suppresses NSCLC proliferation *in vivo* and *in vitro*

MTT assays (A), colony-formation assays (B), EdU assays (C), and flow cytometry analysis (D) were conducted to measure changes in A549 and H1975 cell proliferation and cell cycle after stably infecting Lv-GFP-VPS33B. Student's t test, mean ± SD, *p < 0.05, **p < 0.01. (E) A subcutaneous xenograft mouse model was used to elucidate the function of VPS33B on proliferation. (F and G) Representative H&E and PCNA IHC stainings of subcutaneous tumorigenic tissue are shown.

RESULTS

VPS33B suppresses cell cycle transition and growth

Western blots showed increased VPS33B protein expression after lentiviral particles carrying VPS33B cDNA infected A549 and H1975 cells (Figure S1A). Using 3-(4,5-dimethylthiazol-2-yl)-2,5-diphenyltetrazolium bromide (MTT) assays (Figure 1A), colony formation (Figure 1B; Figure S1B), 5-ethynyl-2′-deoxyuridine (EdU) incorporation assays (Figure 1C; Figure S1C), and cell-cycle analysis (Figure 1D; Figure S1D), we found that overexpressed VPS33B significantly inhibited cell growth and cell-cycle transition in A549 and H1975 cells. We confirmed the inhibition of proliferation by VPS33B *in vivo* with a tumorigenesis study that inoculated VPS33B-overexpressing A549 and H1975 cells into nude mice (Figure 1E). Average weight and volume significantly decreased in VPS33B-overexpressing xenograft mice compared with mock xenograft mice (Figures S1E and S1F). Subcutaneous tumorigenic tissues of nude mice were stained with hematoxylin and eosin (H&E) (Figure 1F). Decreased expression of PCNA was observed in VPS33B-overexpressing tumor tissues compared to control tumor tissues (Figure 1G).

Knocking down VPS33B restored cell growth

Knocking down VPS33B by specific small interfering RNA (siRNA) significantly reduced VPS33B protein expression (Figure 2A) and restored cell growth in VPS33B-overexpressing A549 and H1975 cells

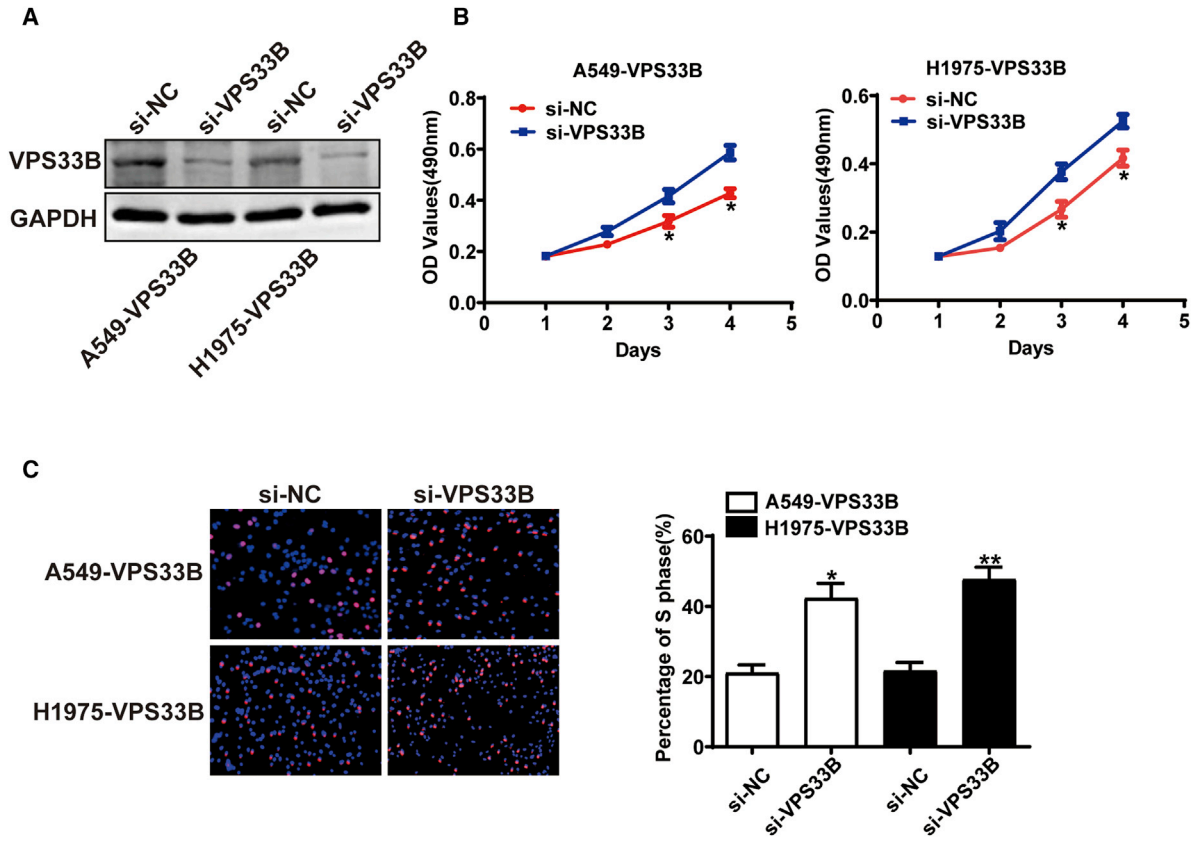

Figure 2. Knocking down VPS33B restored the growth of NSCLC

(A) Western blots were used to examine VPS33B protein expression after knocking down VPS33B by siRNA. GAPDH served as a loading control. MTT assays (B) and EdU incorporation assays (C) were performed after transfecting siRNA against VPS33B in VPS33B-overexpressing A549 and H1975 cells. Student's t test, mean ± SD, *$p < 0.05$, **$p < 0.01$.

by MTT assays (Figure 2B). Suppression of VPS33B also increased EdU staining in VPS33B-overexpressing A549 and H1975 cells (Figure 2C).

miR-192-3p tumor suppressor is induced by VPS33B

We used microRNA (miRNA) chromatin immunoprecipitation (ChIP) assays to detect miRNA expression in A549 VPS33B-overexpressing and control cells. We found that miR-192-3p was notably downregulated in VPS33B-overexpressing A549 cells (Figure 3A) (Table S4). miR-192-3p was upregulated in VPS33B-overexpressing cells compared with empty control cells by qPCR (Figure 3B), which was the inverse of the miRNA ChIP data and suggested the unreliability of miRNA array examination. We also observed that miR-192-3p mimics inhibited proliferation (Figure 3C) and EdU staining (Figure 3D) in NSCLC A549 and H1975 cells.

miR-192-3p directly targets CCNB1

Based on TargetScan and RNA hybrid algorithms, CCNB1 was predicted to be a direct target of miR-192-3p (Figure 4A). Overexpressing miR-192-3p downregulated protein levels of CCNB1 in A549 and H1975 cells (Figure 4B). An miR-192-3p inhibitor upregulated CCNB1 expression in NSCLC cells (Figure 4C). Luciferase reporter assays were used to determine if miR-192-3p directly targeted the untranslated region (3′ UTR) of CCNB1. Cotransfection of miR-192-3p mimics with CCNB1 3′ UTR wild-type vector significantly decreased CCNB1 luciferase reporter activity, while the miR-192-3p inhibitor had the opposite effect. These effects on luciferase activity were not changed when cotransfected with mutant vector (Figure 4D). After transfecting with CCNB1 plasmids, cell growth and EdU staining were restored in miR-192-3p mimic-treated NSCLC cells (Figures 4E and 4F).

miR-192-3p is induced or suppressed by p53 or c-Myc to suppress CCNB1

With the UCSC genome browser (http://genome.ucsc.edu/) and ALGGEN PROMO (http://alggen.lsi.upc.es/cgi-bin/promo_v3/promo/promoinit.cgi?dirDB=TF_8.3), p53 was found to be a putative transcription factor that bound to the promoter of miR-192-3p (Figure 5A). We found that overexpressing p53 increased expression of miR-192-3p using qPCR assays with these cells (Figure 5B). We confirmed that p53 bound to miR-192-3p promoter based on ChIP

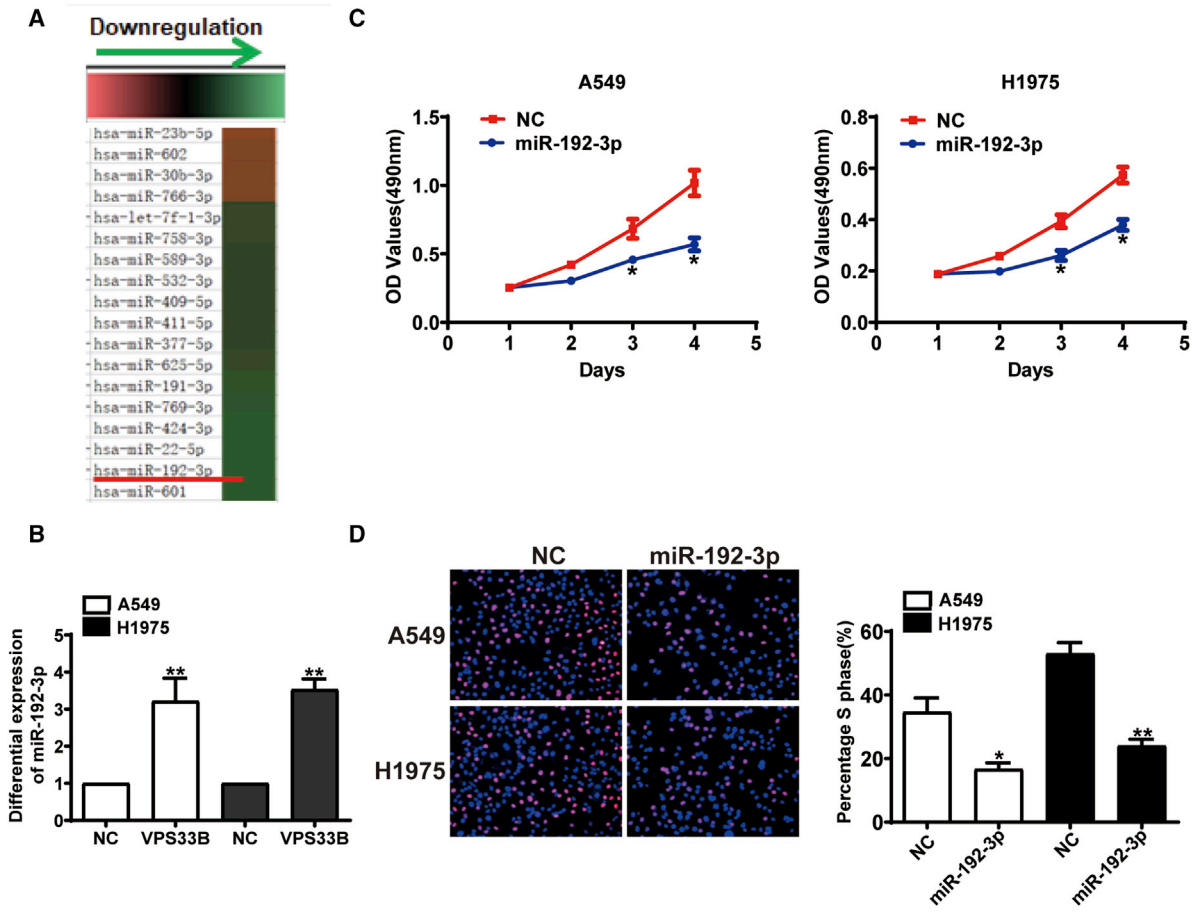

Figure 3. miR-192-3p as tumor suppressor reducing cell growth is induced by VPS33B

(A) miRNA expression profiles were performed in VPS33B-overexpressing A549 cells compared to control cells. Red line indicates the reduced miR-192-3p expression in VPS33B-overexpressing A549 cells. (B) qPCR was used to identify increased expression of miR-192-3p in VPS33B-overexpressing A549 and H1975 cells. Student's t test, mean ± SD, $^{**}p < 0.01$. (C and D) MTT assays and EdU incorporation assays were performed after transfecting miR-192-3p mimics into A549 and H1975 cells. Student's t test, mean ± SD, $^{*}p < 0.05$, $^{**}p < 0.01$.

and gel electrophoresis (Figures 5C and 5D). Promoter activity assays indicated that p53 promoted transcriptional activity of the miR-192-3p promoter (Figure 5E). Overexpression of p53 reduced CCNB1 protein expression and elevated miR-192-3p expression in VPS33B-silencing NSCLC cells (Figures 5F and 5G). H1975 was reported to be a mutant p53 cell line,[17] while no evidence showed whether mutant p53 exert a tumor-suppressive effect in H1975 cells. Western blots showed that specific siRNA for p53 inhibited the expression of p53 protein in H1975 cells (Figure S2A). Knocking down p53 with siRNA promoted cell metastasis and EdU staining (Figures S2B and S2C). These results indicated that p53 still plays a tumor-suppressive role in H1975 cells.

C-Myc was found to be a negative transcription factor of miR-192-3p in HCC cells.[18] Using qPCR assays, we found that overexpressed c-Myc suppressed the expression of miR-192-3p in NSCLC cells (Figure S2D). ChIP assays showed that c-Myc could bind to the promoter of miR-192-3p (Figure S2E). After transfecting miR-192-3p mimics into c-Myc-treated A549 and H1975 cells, the CCNB1 protein level was shown to be decreased (Figure S2F).

Ras/ERK/c-Myc mediated VPS33B to modulate p53/miR-192-3p/CCNB1

Overexpression of c-Myc suppressed p53 and miR-192-3p expression and elevated CCNB1 expression (Figures 6A and 6B). These effects were reversed after transfecting p53 plasmids into VPS33B-overexpressing NSCLC cells with c-Myc treatment (Figures 6A and 6B). Overexpression of c-Myc decreased the combination of p53 with the miR-192-3p promoter (Figure 6C), and p53 transfection restored the binding of p53 to the miR-192-3p promoter in VPS33B-overexpressing cells (Figure 6C). We observed that overexpressing VPS33B increased p53 and miR-192-3p levels and decreased KRas, p-ERK1/2, c-Myc, and CCNB1 expression (Figures 6D and 6E), while overexpressing KRas had the inverse effects (Figures S3A and S3B). These effects of VPS33B were reversed after transfecting KRas plasmids into NSCLC cells with VPS33B (Figures 6D and 6E). VPS33B

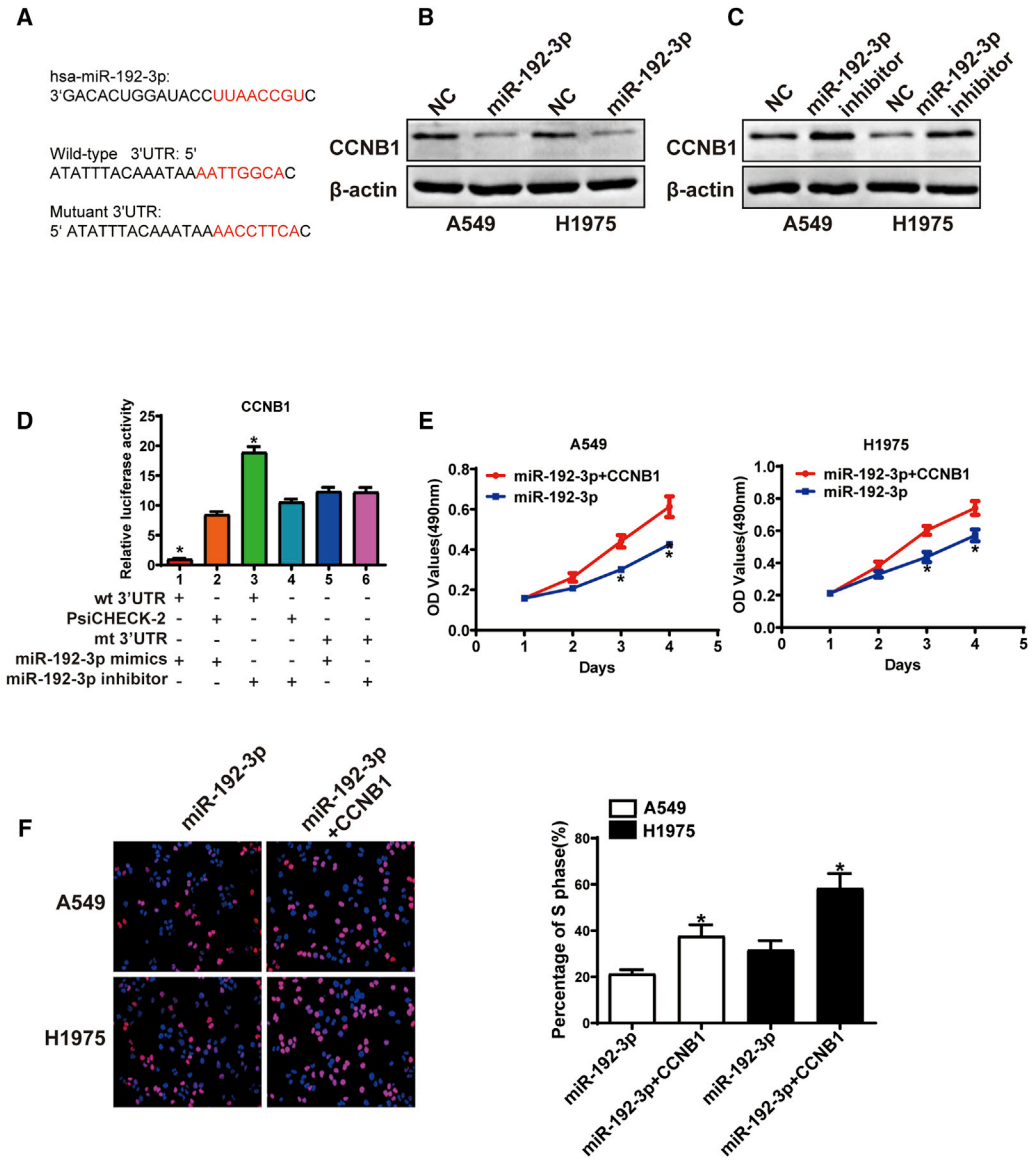

Figure 4. miR-192-3p directly regulates cyclin B1 (CCNB1)

(A) Bioinformatics analysis was used to predict miR-192-3p-binding sequences within the 3′ UTR region of CCNB1. (B and C) CCNB1 protein expression in the A549 and H1975 cells transfected with miR-192-3p mimics or inhibitor was detected by western blots. β-actin served as a loading control. (D) That miR-192-3p directly targets CCNB1 was confirmed by luciferase reporter assays. One-way ANOVA, mean ± SD, *p < 0.05. (E and F) MTT assays and EdU assays were conducted after transfecting with CCNB1 plasmids in miR-192-3p mimic-treated A549 and H1975 cells. Student's t test, mean ± SD, *p < 0.05.

overexpression increased the combination of p53 with the miR-192-3p promoter (Figure 6F), and KRas transfection decreased the binding of p53 to miR-192-3p the promoter in NSCLC cells (Figure 6F).

Decreased VPS33B expression as an unfavorable outcome

VPS33B protein staining was in the cell cytoplasm (Figure 7A). Compared to the bronchial epithelia of lung tissues, VPS33B protein levels were significantly reduced in NSCLC tissues ($p < 0.001$) (Table 1). We observed that reduced VPS33B protein expression significantly correlated with T classification (T_1–T_2 versus T_3–T_4, χ^2, p = 0.013), N classification (N_0 versus N_1–N_3, χ^2, p = 0.002), pathological classification (1–2 versus 3, χ^2, p = 0.007) (1 = well differentiated, 2 = moderately differentiated, 3 = poorly differentiated), and AJCC stage (I–II versus III–IV, χ^2, p = 0.008), but no other clinical features (Table 2). Survival analysis showed that reduced VPS33B protein expression was associated with poor prognosis of patients with NSCLC (p = 0.001) (Figure 7B). The lower the VPS33B protein expression was, the shorter the overall survival time was. Stratum analysis indicated that reduced VPS33B protein levels caused a tendency for shorter survival time with early- or advanced-stage

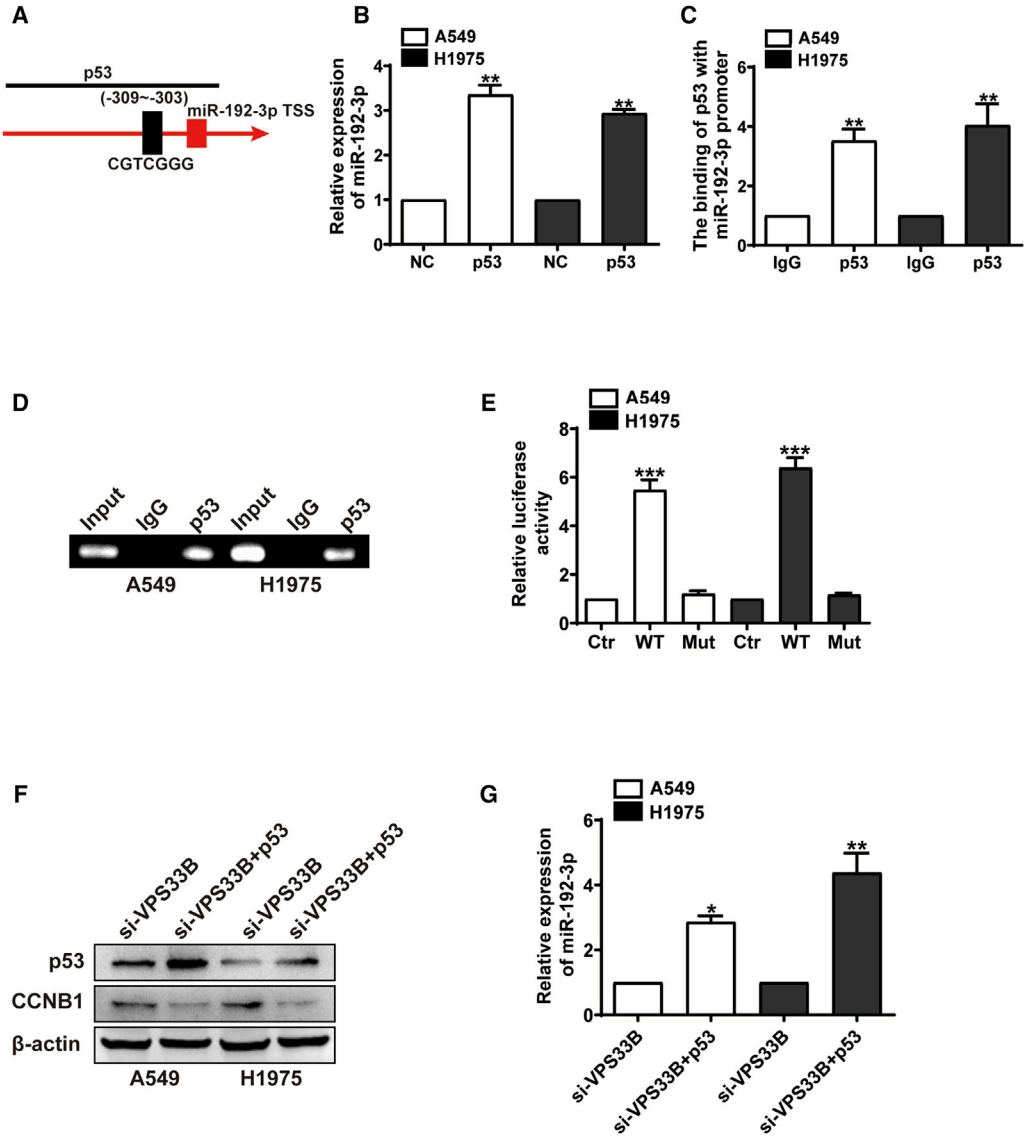

Figure 5. p53 induces miR-192-3p expression by binding to its promoter region to suppress CCNB1

(A) Bioinformatics analysis predicted the putative p53 binding site of the promoter region of miR-192-3p. (B) qPCR assays were performed to determine miR-192-3p expression in the p53-overexpressing A549 and H1975 cells. Student's t test, mean ± SD, **p < 0.01. qPCR (C) and gel electrophoresis (D) were used to confirm the amplification of p53-binding sites after ChIP using antibody against p53. Immunoglobulin G (IgG) antibody was used as the negative control. Student's t test, mean ± SD, **p < 0.01. (E) Luciferase reporter assays were used to demonstrate the luciferase activities of the wild-type and mutant miR-192-3p promoter in A549 and H1975 cells transfected with the p53 plasmid. One-way ANOVA, mean ± SD, ***p < 0.001. (F) The expression of CCNB1 was shown in VPS33B-silencing A549 and H1975 cells with the transfection of the p53 plasmid by western blots. β-actin served as a loading control. (G) The differential expression of miR-192-3p was shown in VPS33B-silencing A549 and H1975 cells after transfecting the p53 plasmid by qPCR. Student's t test, mean ± SD, *p < 0.05, **p < 0.01.

NSCLC (Figure 7C). Cox regression analysis demonstrated that T and N classifications were independent prognostic factors for patients with NSCLC (Table 3).

DISCUSSION

In previous studies, VPS33B was reported as a tumor suppressor participating in the pathogenesis of HCC, NPC, colon cancer, and lung adenocarcinoma. However, its effect in NSCLC has never been documented. We observed that the VPS33B protein was significantly downregulated in NSCLC tissues compared to lung bronchial epithelium tissues by immunochemical staining assays. Furthermore, reduced VPS33B protein expression promoted progression, which was an unfavorable factor and led to a poor prognosis for NSCLC patients. These data supported our previous studies on VPS33B in NPC and colon cancer,[14,15] which indicated that VPS33B acts as a tumor suppressor in NSCLC.

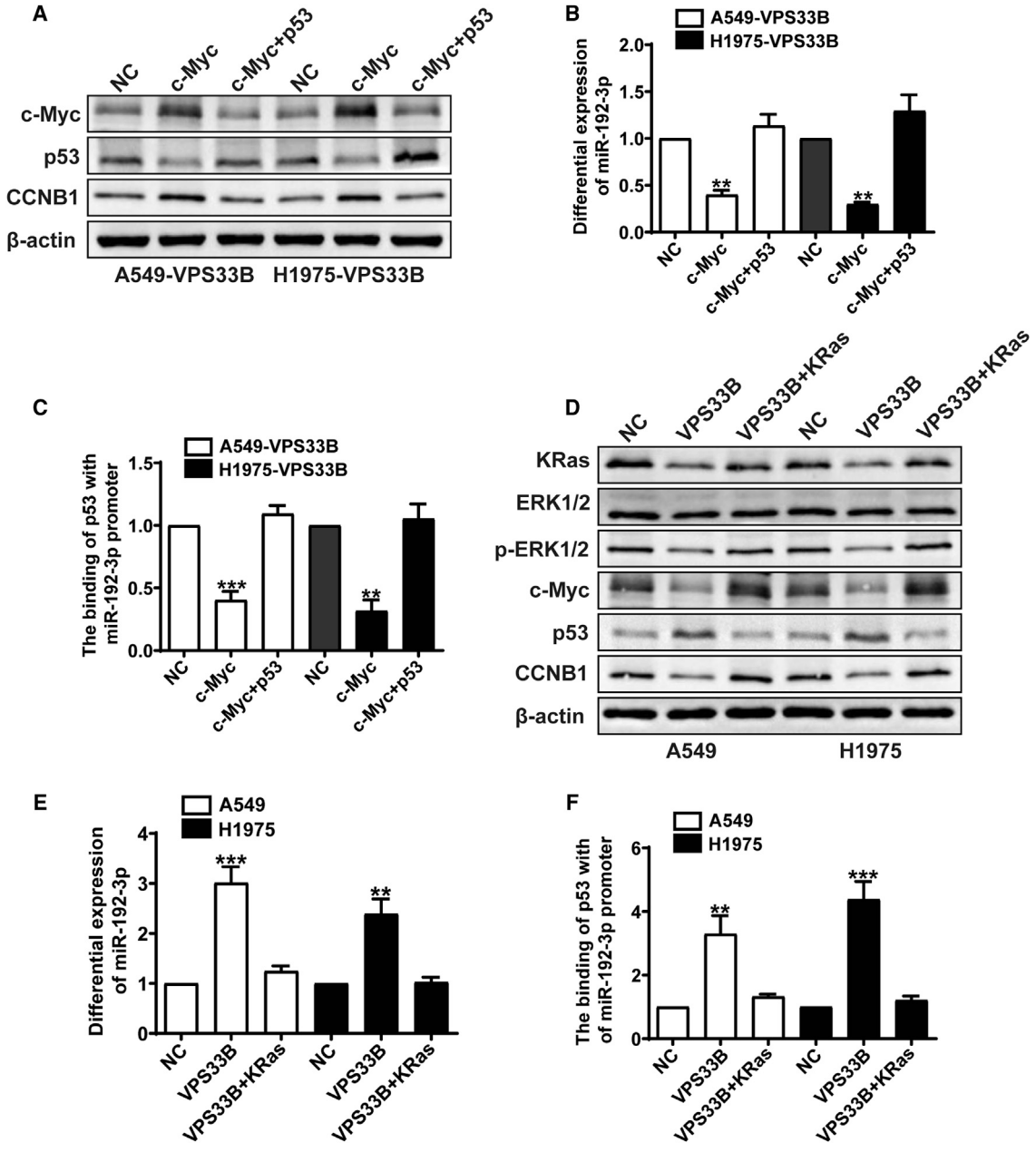

Figure 6. VPS33B modulates p53/miR-192-3p/CCNB1 through Ras/ERK/c-Myc signal

(A) Changes in c-Myc, p53, and CCNB1 expression were detected by western blot analysis in VPS33B-overexpressing A549 and H1975 cells after transfection of c-Myc or c-Myc+p53 plasmids. β-actin was used as a loading control. (B and C) The expression of miR-192-3p and the binding of p53 with miR-192-3p promoter were detected in VPS33B-overexpressing A549 and H1975 cells after transfecting c-Myc or c-Myc+p53 plasmids by qPCR or ChIP-qPCR assays. One-way ANOVA, mean ± SD, $^{**}p < 0.01$,$^{***}p < 0.001$. (D) Expression changes of Ras/ERK/p-ERK, c-Myc, p53, and CCNB1 proteins were detected by western blot analysis in A549 and H1975 cells after transfecting VPS33B or VPS33B+KRas plasmids. β-actin was used as a loading control. (E and F) qPCR or ChIP-qPCR assays were used to detect the expression of miR-192-3p and the binding of p53 with miR-192-3p promoter in A549 and H1975 cells with the transfection of VPS33B or VPS33B+KRas plasmids. One-way ANOVA, mean ± SD, $^{**}p < 0.01$,$^{***}p < 0.001$.

After constructing stable VPS33B-overexpressing NSCLC cell lines, we observed that increased VPS33B significantly reduced cell cycle progression and cell proliferation by a series of *in vitro* and *in vivo* experiments. After knocking down VPS33B expression, cell growth and cell cycle transition were significantly restored. These data supported VPS33B as a tumor suppressor in NSCLC, which was consistent with our previous reports on NPC and colon cancer.

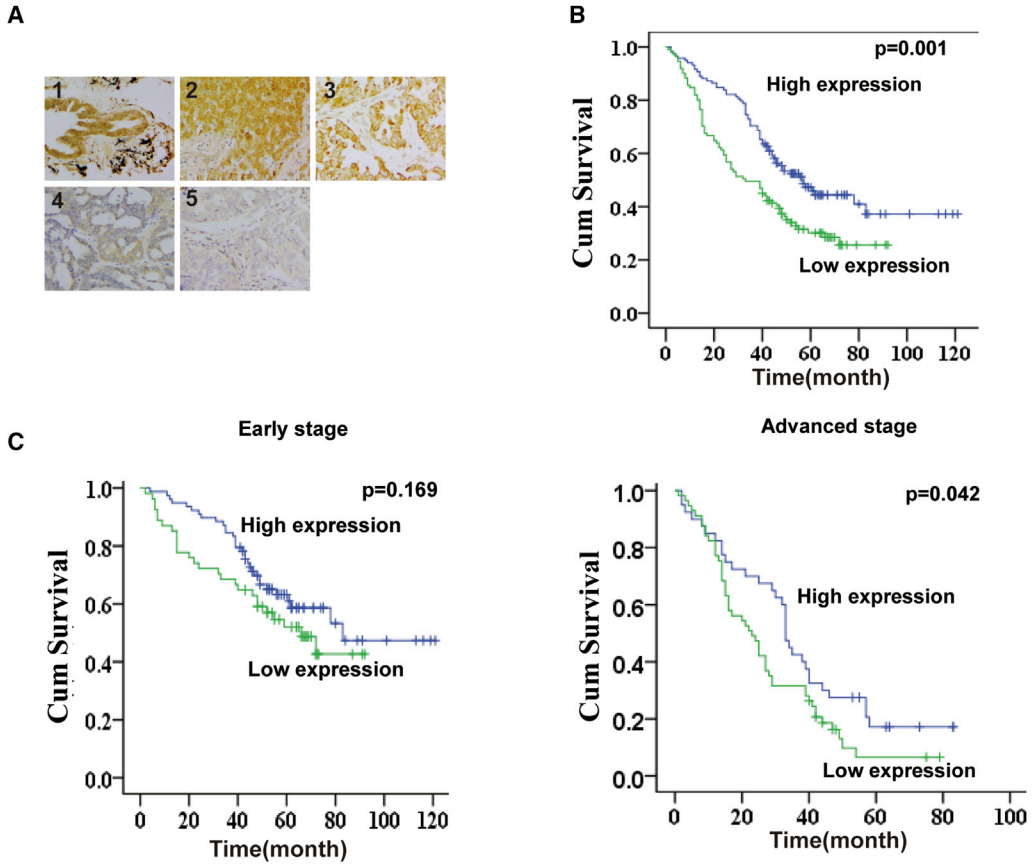

Figure 7. VPS33B downregulation is an unfavorable factor in NSCLC

(A) VPS33B protein expression was examined in bronchial epithelial of lung tissues and NSCLC samples. (1) High VPS33B expression in bronchial epithelium of lung tissue; (2 and 3) high VPS33B expression in NSCLC tissues; (4 and 5) low VPS33B expression in NSCLC tissues. (B) Kaplan-Meier survival analysis based on VPS33B expression. Log-rank test was used to calculate p values. (C) Stratum analysis of overall survival based on AJCC stage.

In previous studies, miRNAs were shown to be mediators in the pathogenesis of tumors including lung cancer, liver cancer, and NPC.[19–22] We observed that, for NPC and lung adenocarcinoma, miR-3188 directly targeted mTOR, miR-374a targeted CCND1, and miR-296-3p targeted PRKCA to respectively participate in FOXO1, PDCD4, and HDGF-mediated modulation of malignant phenotypes.[5,23–26] In this study, we examined VPS33B-modulated miRNA expression profiles by miRNA arrays and found that miR-192-3p was downregulated in VPS33B-overexpressing NSCLC. However, real-time PCR results demonstrated that miR-192-3p expression was markedly elevated in VPS33B-overexpressing NSCLC, which suggested that the reliability of miRNA arrays was not perfect.

In a previous study, miR-192-3p was reported as a tumor prognosis marker of colorectal cancer that only suppressed farnesoid X receptor (FXR) in tumor pathogenesis.[27,28] However, the miR-192-3p function is still unclear in tumors, including NSCLC. In this investigation, we observed that miR-192-3p suppressed tumor cell proliferation and cell cycle transition in NSCLC. Furthermore, bioinformatics assays predicted that CCNB1 is a target of miR-192-3p. CCNB1 is a regulatory protein involved in mitosis and is a critical cell cycle regulator of the G_2/M checkpoint. Previous studies showed that CCNB1 is an oncogene that participates in the pathogenesis of a variety of cancers such as breast cancer, NPC, colorectal cancer, NSCLC, and colon, prostate, oral, and esophageal cancer.[29–35] High expression is usually found before tumor cells become immortalized and aneuploid, which can contribute to chromosomal instability and the aggressive nature of certain cancers. These data demonstrate the importance of CCNB1 in tumor pathogenesis, including NSCLC. In further experiments, we confirmed the binding of miR-192-3p to the 3′ UTR of CCNB1 and subsequent decrease in CCNB1 expression. Overexpression of CCNB1 reversed the suppressive effects on miR-192-3p in NSCLC cell growth and EdU staining.

p53 is a classic tumor-suppressive transcription factor involved in the transcription modulation of many genes, including miRNAs.[36–40] Interestingly, bioinformatics predictions indicated a p53 binding site in the miR-192-3p promoter region. In accordance with the prediction, experiments confirmed the binding of p53 to the miR-192-3p promoter, followed by the induced expression of miR-192-3p that

Table 1. The expression of VPS33B in NSCLC compared to non-cancerous lung tissues

		VPS33B expression		
Group	Cases (n)	High expression	Low expression	p value
Cancer	229	118	111	$p < 0.001$
Bronchial epithelium	42	33	9	

χ^2 test was applied to access the expression of NSCLC and normal lung tissues.

reduced CCNB1 expression. These data demonstrated a p53/miR-192-3p/CCNB1 pathway in NSCLC pathogenesis. In addition, we also found that c-Myc was a transcription factor binding to the promoter of miR-192-3p and negatively modulated its expression and thus elevated CCNB1 expression in NSCLC.

In a previous study, we observed that VPS33B suppressed Ras/ERK-stimulated expression of c-Myc and, therefore, upregulated p53 expression in colon cancer. We hypothesized that VPS33B modulated p53/miR-192-3p/CCNB1 signaling, possibly via suppressing the Ras/ERK/c-Myc pathway. To test this hypothesis, we separately transfected c-Myc and KRas plasmids into VPS33B-overexpressing NSCLC cells and observed that p53/miR-192-3p/CCNB1 signaling was clearly reversed. These data were consistent with our hypothesis.

In summary, we observed that expression of VPS33B protein was downregulated in NSCLC compared to lung bronchial epithelial tissue. Furthermore, reduced VPS33B protein expression led to poor prognosis for patients with NSCLC. Finally, mechanism analysis indicated that VPS33B regulated c-Myc/p53/miR-192-3p to target CCNB1 by inactivating Ras/ERK signaling, thereby suppressing growth in NSCLC. Our data demonstrated that VPS33B is tumor suppressive in NSCLC pathogenesis.

MATERIALS AND METHODS

Cell culture

NSCLC A549 and H1975 cell lines were purchased from the cell bank for a typical culture preservation committee of the Chinese Academy of Sciences and were maintained in RPMI 1640 supplemented with 10% newborn calf serum (ExCell, Shanghai, China) in a humidified chamber with 5% CO_2 at 37°C. Cell lines were confirmed to be free of mycoplasma contamination.

Lentivirus infection

Lentiviral particles carrying VPS33B cDNA and GFP vector were from GeneChem (Shanghai, China) and were used to infect A549 and H1975 cells. VPS33B protein was measured using western blots.

RNA isolation, reverse transcription, and qPCR

RNA isolation, reverse transcription, and qPCR were performed on NSCLC cell lines according to instructions of a Trizol and Takara qRT-PCR kit (Takara Bio, Shiga, Japan). Specific sense primers for miR-192-3p and U6 were shown in Table S1.

Cell proliferation and colony-formation assays

MTT assays were used to examine cell viability. Cells (1,000/well) were seeded in 96-well plates. For lentivirus-mediated VPS33B overexpression, cells were incubated for 1, 2, 3, 4, 5, 6, or 7 days. For transient transfection with siRNA for VPS33B plasmids, miR-192-3p mimics, miR-192-3p inhibitor, or CCNB1 plasmids, cells were cultured for 1, 2, 3, or 4 days. Subsequently, 20 mL MTT solution (5 mg/mL in PBS) (Sigma, St. Louis, MO, USA) was added to each well and incubated for 4 h. Formazan crystals formed by viable cells were solubilized in 150 mL dimethyl sulfoxide (Sigma, St. Louis, MO, USA), and absorbance (OD) was measured at 490 nm. For colony-formation assays, NSCLC cells with lentivirus-mediated VPS33B overexpression were seeded in 6-well culture plates at 100 cells/well with 2 wells per group. After incubation for 14 days at 37°C, colonies were washed twice with PBS and stained with hematoxylin solution. Colonies of more than 50 cells were counted under a microscope. All experiments were repeated at least three times.

Cell cycle and EdU incorporation

Cell cycle and EdU incorporation assays were performed as previously described.[24] For cell cycle analysis, 5×10^6 NSCLC cells were harvested after 48 h incubation and washed with cold PBS. Cells were fixed with 70% ice-cold ethanol at 4°C overnight, after incubation with PBS containing 10 mg/mL propidium iodide and 0.5 mg/mL RNase A for 15 min at 37°C. Fixed cells were washed with cold PBS three times. Fluorescence-activated cell sorting (FACS) caliber flow cytometry (BD Biosciences) was used to determine DNA content of labeled cells. For EdU incorporation assays, proliferating NSCLC cells were examined using cell-light EdU Apollo 488 or 567 *in vitro* imaging kits (RiboBio) according to the manufacturer's protocol. After incubation with 10 mM EdU for 2 h, NSCLC cells were fixed with 4% paraformaldehyde, permeabilized in 0.3% Triton X-100, and stained with Apollo fluorescent dyes, with 5 μg/mL DAPI used to stain cell nuclei for 10 min. The number of EdU-positive cells was counted under a fluorescent microscope in five random fields. All assays were independently performed three times.

In vivo tumorigenesis in nude mice

For *in vivo* tumorigenesis assays, 1×10^6 logarithmically growing VPS33B-overexpressing A549 and H1975 cells or control parental cells in 0.1 mL RPMI 1640 medium were subcutaneously injected into the left or right flank of 4-week-old 11- to 12-g male BALB/c nu/nu mice (N = 5). After 18 days, mice were killed and tumor tissues were excised and weighed. Mice were maintained in a barrier facility on HEPA-filtered racks and fed with an autoclaved laboratory rodent diet. All animal studies were conducted in accordance with the principles and procedures outlined in Guangzhou Medical University Guide for the Care and Use of Animals.

Transient transfection with siRNAs, plasmids, and miR-192-3p mimics and inhibitor

miR-192-3p mimics, miR-192-3p inhibitor, siRNA for VPS33B, and p53 were designed and synthesized at RiboBio (Guangzhou, China). VPS33B plasmids were built by our team. c-Myc, KRas, and p53

Table 2. Correlation between the clinicopathologic characteristics and VPS33B expression in NSCLC

		VPS33B expression		
Factors	n	Low (n)	High (n)	p value
Gender				
Male	99	43	56	p = 0.183
Female	130	68	62	
Age (y)				
≤60	101	46	55	p = 0.431
>60	128	65	63	
T classification				
T_1–T_2	164	71	93	p = 0.013
T_3–T_4	65	40	25	
N classification				
N_0	141	57	84	p = 0.002
N_1–N_3	88	54	34	
M classification				
M_0	225	109	116	p = 0.951
M_1	4	2	2	
Pathological classification				
1–2	152	64	88	p = 0.007
3	77	47	30	
AJCC stage				
I–II	132	54	78	p = 0.008
III–IV	97	57	40	

χ^2 test was applied to access the correlation between the clinicopathologic characteristics and VPS33B expression.

plasmids were from Vigenebio (Shandong, China). At 24 h before transfection, A549 and H1975 cells were plated onto 6-well or 96-well plates (Nest Biotech, China) at 30%–50% confluence. Plasmids, siRNAs, mimics, and inhibitor (Table S2) were used for transfections at a working concentration of 100 nM using TurboFect siRNA transfection reagent (Fermentas, Vilnius, Lithuania) according to the manufacturer's protocol. Cells were collected after 48–72 h for experiments.

Western blot analysis, reagent, and antibodies

Western blots were as described[41] with primary antibodies against VPS33B, ERK, p-ERK, KRas, CCNB1, c-Myc, and p53. β-actin and GAPDH were loading controls for all blots. Dilutions and sources of antibodies are in Table S3. Images were captured with the Minichemi chemiluminescence imaging system (Beijing Sage Creation Science, China).

Immunohistochemistry (IHC)

Immunohistochemistry was as previously described.[41] Tissue arrays for lung adenocarcinoma were from Shanghai Outdo Biotech (Shanghai, China). To use these clinical materials for research purposes, prior consent was obtained from patients and the Ethics Committees of Taizhou Hospital, Zhejiang, China. Sections were visualized with 3,3'-diaminobenzidine (DAB) and counterstained with hematoxylin, mounted in neutral gum, and analyzed using a bright field microscope.

A staining index (range 0 to 7) was determined by VPS33B staining intensity (0 = negative, 1 = weakly positive, 2 = moderately positive, 3 = strongly positive) and proportion of immunopositive tumor cells (< 10% = 1, 10% to < 50% = 2, 50% to < 75% = 3, ≥ 75% = 4). A score of 6 or higher was classified as high expression, and less than 6 was low expression.

miRNA array following overexpressed VPS33B

miRNA arrays were by Gene Co. (Shanghai, China). Affymetrix gene ChIP micro 2.0 arrays (Affymetrix, Santa Clara, CA, USA) that provide 100% miRBase v17 coverage (www.mirbase.org) by a one-color approach were employed for universal miRNA coverage. Total RNA (6–7 mg) was isolated from VPS33B and control A549 cells. Statistical analysis used the open source R software (http://www.r-project.org)

Luciferase reporter assays

CCNB1 was predicted to be a target of miR-192-3p using TargetScan software. Fragments of the CCNB1 3′ UTR amplified by PCR primers were cloned into psiCHECK-2 vectors (wild-type 3′ UTR). Site-directed mutagenesis of the miR-192-3p binding sites in the CCNB1 3′ UTR (mutant-type 3′ UTR) was by GeneTailor site-directed mutagenesis system (Invitrogen). For reporter assays, wild-type or mutant vector and control vector psiCHECK-2 vector were cotransfected into A549 cells with miR-192-3p mimics or inhibitor. Luciferase activity was measured at 48 h after transfection using a dual-luciferase reporter assay system (Promega, Madison, WI, USA). To examine the effect of p53 on miR-192-3p promoter activity, fragments containing a p53 binding site were cloned into the pGL3-basic luciferase reporter vector, and p53 binding site mutation vectors were constructed. These p53 plasmids were cotransfected into A549 and H1975 cells. Luciferase reporter activity of the miR-192-3p promoter was measured at 48 h after transfection.

ChIP assay

ChIP assays were performed to examine if p53 and c-Myc bound the miR-192-3p promoter using a kit (Millipore). A549 and H1975 cells with or without lentiviral-mediated ectopic VPS33B expression were fixed with 1% formaldehyde to covalently crosslink proteins to DNA, and chromatin was harvested from the selected cells. Crosslinked DNA was sheared to 200–1,000 base pairs with sonication and subjected to immmmunoselection with anti-c-Myc or p53. To measure enrichment of DNA fragments at the binding site in the miR-192-3p promoter, qPCR was used with specific primers.

Statistical analysis

Statistical analyses were performed with the SPSS 22.0 statistical software package (SPSS, Chicago, IL, USA) and GraphPad Prism v5.0 (GraphPad Software, La Jolla, CA, USA) software. Data are expressed as mean ± SD from at least three independent experiments.

Table 3. Univariate and multivariate Cox regression analysis in 229 NSCLC patients

	Univariate analysis			Multivariate analysis		
Parameters	HR	95% CI	p value*	HR	95% CI	p value*
VPS33B expression						
Low versus high expression	0.582	0.417–0.813	0.002	0.733	0.515–1.042	0.084
Sex						
Male versus female	1.341	0.955–1.881	0.090			
Age (y)						
<60 versus ≥60	1.167	0.835–1.633	0.366			
T classification						
T_1–T_2 versus T_3–T_4	2.242	1.582–3.178	0.000	1.503	1.026–2.201	0.036
N classification						
N_0 versus N_1–N_3	3.715	2.636–5.236	0.000	2.574	1.050–6.310	0.039
M classification						
M_0 versus M_1	2.053	0.757–5.569	0.158	0.902	0.326–2.493	0.842
AJCC stage						
I–II versus III–IV	3.485	2.468–4.921	0.000	1.300	0.515–3.279	0.579
Pathological classification						
1–2 versus 3	1.320	0.938–1.858	0.111	0.901	0.627–1.293	0.570

*$p < 0.05$ statistically significant. T, tumor size; N, lymph node; M, distant metastasis; HR, hazard ratio; 95% CI, 95% confidence interval.

Differences were considered to be statistically significant at $p < 0.05$ by Student's t test for two groups and one-way ANOVA analysis for multiple groups. Kaplan-Meier curves were used for survival analysis, and a Cox proportional hazard regression model was used to identify independent prognostic factors.

SUPPLEMENTAL INFORMATION

Supplemental Information can be found online at https://doi.org/10.1016/j.omtn.2020.11.010.

ACKNOWLEDGMENTS

We thank International Science Editing (https://www.internationalscienceediting.com) for editing this manuscript. This study was supported by the National Natural Science Foundation of China (no. 81572247), the Natural Science Foundation of Guangdong Province (nos. 2017A030313702 and 2015A030311005), the Shenzhen Health System Science Foundation (no. SZBC2018019), the Supporting Plan for Special Talents in Guangdong Province (no. 2016TQ03R466), the Guangzhou Science and Technology Program key projects (no. 201804010023), and the Natural Science Foundation of Hainan Province (no. 819QN358).

AUTHOR CONTRIBUTIONS

G.Y., J.J., Z.L., and R.L. conceived and designed the experiments; J.L., P.X., Y.W., S.L., Y.X., S.D., and S.H. performed the experiments; J.L. and G.Y. analyzed the data; J.J. wrote the paper.

DECLARATION OF INTERESTS

The authors declare no competing interests.

REFERENCES

1. Guo, J., Wang, X., Wang, Y., Wang, L., and Hua, S. (2019). A promising role of interferon regulatory factor 5 as an early warning biomarker for the development of human non-small cell lung cancer. Lung Cancer *135*, 47–55.
2. Yang, L., Dong, Y., Li, Y., Wang, D., Liu, S., Wang, D., Gao, Q., Ji, S., Chen, X., Lei, Q., et al. (2019). IL-10 derived from M2 macrophage promotes cancer stemness via JAK1/STAT1/NF-κB/Notch1 pathway in non-small cell lung cancer. Int. J. Cancer *145*, 1099–1110.
3. Hu, Y., Wei, X., Lv, Y., Xie, X., Yang, L., He, J., Tao, X., Ma, Y., Su, Y., Wu, L., et al. (2020). EIF3H interacts with PDCD4 enhancing lung adenocarcinoma cell metastasis. Am. J. Cancer Res. *10*, 179–195.
4. Yuan, M., Huang, L.L., Chen, J.H., Wu, J., and Xu, Q. (2019). The emerging treatment landscape of targeted therapy in non-small-cell lung cancer. Signal Transduct. Target. Ther. *4*, 61.
5. Zhao, M., Xu, P., Liu, Z., Zhen, Y., Chen, Y., Liu, Y., Fu, Q., Deng, X., Liang, Z., Li, Y., et al. (2018). Dual roles of miR-374a by modulated c-Jun respectively targets CCND1-inducing PI3K/AKT signal and PTEN-suppressing Wnt/β-catenin signaling in non-small-cell lung cancer. Cell Death Dis. *9*, 78.
6. Jin, M., Shi, C., Yang, C., Liu, J., and Huang, G. (2019). Upregulated circRNA ARHGAP10 Predicts an Unfavorable Prognosis in NSCLC through Regulation of the miR-150-5p/GLUT-1 Axis. Mol. Ther. Nucleic Acids *18*, 219–231.
7. Xu, T., Yan, S., Jiang, L., Yu, S., Lei, T., Yang, D., Lu, B., Wei, C., Zhang, E., and Wang, Z. (2019). Gene Amplification-Driven Long Noncoding RNA SNHG17 Regulates Cell Proliferation and Migration in Human Non-Small-Cell Lung Cancer. Mol. Ther. Nucleic Acids *17*, 405–413.
8. Zhu, H., Chang, L.L., Yan, F.J., Hu, Y., Zeng, C.M., Zhou, T.Y., Yuan, T., Ying, M.D., Cao, J., He, Q.J., and Yang, B. (2018). AKR1C1 Activates STAT3 to Promote the Metastasis of Non-Small Cell Lung Cancer. Theranostics *8*, 676–692.
9. Yao, G., Chen, K., Qin, Y., Niu, Y., Zhang, X., Xu, S., Zhang, C., Feng, M., and Wang, K. (2019). Long Non-coding RNA JHDM1D-AS1 Interacts with DHX15 Protein to Enhance Non-Small-Cell Lung Cancer Growth and Metastasis. Mol. Ther. Nucleic Acids *18*, 831–840.
10. Vyse, S., and Huang, P.H. (2019). Targeting *EGFR* exon 20 insertion mutations in non-small cell lung cancer. Signal Transduct. Target. Ther. *4*, 5.
11. Ke, B., Wei, T., Huang, Y., Gong, Y., Wu, G., Liu, J., Chen, X., and Shi, L. (2019). Interleukin-7 Resensitizes Non-Small-Cell Lung Cancer to Cisplatin via Inhibition of ABCG2. Mediators Inflamm. *2019*, 7241418.
12. Carim, L., Sumoy, L., Andreu, N., Estivill, X., and Escarceller, M. (2000). Cloning, mapping and expression analysis of VPS33B, the human orthologue of rat Vps33b. Cytogenet. Cell Genet. *89*, 92–95.
13. Wang, C., Cheng, Y., Zhang, X., Li, N., Zhang, L., Wang, S., Tong, X., Xu, Y., Chen, G.Q., Cheng, S., et al. (2018). Vacuolar Protein Sorting 33B Is a Tumor Suppressor in Hepatocarcinogenesis. Hepatology *68*, 2239–2253.
14. Chen, Y., Liu, Z., Wang, H., Tang, Z., Liu, Y., Liang, Z., Deng, X., Zhao, M., Fu, Q., Li, L., et al. (2020). VPS33B negatively modulated by nicotine functions as a tumor suppressor in colorectal cancer. Int. J. Cancer *146*, 496–509.
15. Liang, Z., Liu, Z., Cheng, C., Wang, H., Deng, X., Liu, J., Liu, C., Li, Y., and Fang, W. (2019). VPS33B interacts with NESG1 to modulate EGFR/PI3K/AKT/c-Myc/P53/

miR-133a-3p signaling and induce 5-fluorouracil sensitivity in nasopharyngeal carcinoma. Cell Death Dis. *10*, 305.

16. Liu, Z., Liu, J., Li, Y., Wang, H., Liang, Z., Deng, X., Fu, Q., Fang, W., and Xu, P. (2020). VPS33B suppresses lung adenocarcinoma metastasis and chemoresistance to cisplatin. Genes Dis. Published online January 8, 2020. https://doi.org/10.1016/j.gendis.2019.12.009.

17. Van den Bossche, J., Deben, C., De Pauw, I., Lambrechts, H., Hermans, C., Deschoolmeester, V., Jacobs, J., Specenier, P., Pauwels, P., Vermorken, J.B., et al. (2019). In vitro study of the Polo-like kinase 1 inhibitor volasertib in non-small-cell lung cancer reveals a role for the tumor suppressor p53. Mol. Oncol. *13*, 1196–1213.

18. Wang, J., Chen, J., Liu, Y., Zeng, X., Wei, M., Wu, S., Xiong, Q., Song, F., Yuan, X., Xiao, Y., et al. (2019). Hepatitis B Virus Induces Autophagy to Promote its Replication by the Axis of miR-192-3p-XIAP Through NF kappa B Signaling. Hepatology *69*, 974–992.

19. Lin, X., Zuo, S., Luo, R., Li, Y., Yu, G., Zou, Y., Zhou, Y., Liu, Z., Liu, Y., Hu, Y., et al. (2019). HBX-induced miR-5188 impairs FOXO1 to stimulate β-catenin nuclear translocation and promotes tumor stemness in hepatocellular carcinoma. Theranostics *9*, 7583–7598.

20. Zhang, W.C., Chin, T.M., Yang, H., Nga, M.E., Lunny, D.P., Lim, E.K., Sun, L.L., Pang, Y.H., Leow, Y.N., Malusay, S.R., et al. (2016). Tumour-initiating cell-specific miR-1246 and miR-1290 expression converge to promote non-small cell lung cancer progression. Nat. Commun. *7*, 11702.

21. Li, Y., Lv, Y., Cheng, C., Huang, Y., Yang, L., He, J., Tao, X., Hu, Y., Ma, Y., Su, Y., et al. (2020). SPEN induces miR-4652-3p to target HIPK2 in nasopharyngeal carcinoma. Cell Death Dis. *11*, 509.

22. Liu, Y., Jiang, Q., Liu, X., Lin, X., Tang, Z., Liu, C., Zhou, J., Zhao, M., Li, X., Cheng, Z., et al. (2019). Cinobufotalin powerfully reversed EBV-miR-BART22-induced cisplatin resistance via stimulating MAP2K4 to antagonize non-muscle myosin heavy chain IIA/glycogen synthase 3β/β-catenin signaling pathway. EBioMedicine *48*, 386–404.

23. Deng, X., Liu, Z., Liu, X., Fu, Q., Deng, T., Lu, J., Liu, Y., Liang, Z., Jiang, Q., Cheng, C., and Fang, W. (2018). miR-296-3p Negatively Regulated by Nicotine Stimulates Cytoplasmic Translocation of c-Myc via MK2 to Suppress Chemotherapy Resistance. Mol. Ther. *26*, 1066–1081.

24. Zhao, M., Luo, R., Liu, Y., Gao, L., Fu, Z., Fu, Q., Luo, X., Chen, Y., Deng, X., Liang, Z., et al. (2016). miR-3188 regulates nasopharyngeal carcinoma proliferation and chemosensitivity through a FOXO1-modulated positive feedback loop with mTOR-p-PI3K/AKT-c-JUN. Nat. Commun. *7*, 11309.

25. Zhen, Y., Fang, W., Zhao, M., Luo, R., Liu, Y., Fu, Q., Chen, Y., Cheng, C., Zhang, Y., and Liu, Z. (2017). miR-374a-CCND1-pPI3K/AKT-c-JUN feedback loop modulated by PDCD4 suppresses cell growth, metastasis, and sensitizes nasopharyngeal carcinoma to cisplatin. Oncogene *36*, 275–285.

26. Fu, Q., Song, X., Liu, Z., Deng, X., Luo, R., Ge, C., Li, R., Li, Z., Zhao, M., Chen, Y., et al. (2017). miRomics and Proteomics Reveal a miR-296-3p/PRKCA/FAK/Ras/c-Myc Feedback Loop Modulated by HDGF/DDX5/β-catenin Complex in Lung Adenocarcinoma. Clin. Cancer Res. *23*, 6336–6350.

27. Slattery, M.L., Herrick, J.S., Mullany, L.E., Wolff, E., Hoffman, M.D., Pellatt, D.F., Stevens, J.R., and Wolff, R.K. (2016). Colorectal tumor molecular phenotype and miRNA: expression profiles and prognosis. Mod. Pathol. *29*, 915–927.

28. Krattinger, R., Boström, A., Schiöth, H.B., Thasler, W.E., Mwinyi, J., and Kullak-Ublick, G.A. (2016). microRNA-192 suppresses the expression of the farnesoid X receptor. Am. J. Physiol. Gastrointest. Liver Physiol. *310*, G1044–G1051.

29. Ohta, T., Okamoto, K., Isohashi, F., Shibata, K., Fukuda, M., Yamaguchi, S., and Xiong, Y. (1998). T-loop deletion of CDC2 from breast cancer tissues eliminates binding to cyclin B1 and cyclin-dependent kinase inhibitor p21. Cancer Res. *58*, 1095–1098.

30. Wang, J., Chang, L., Lai, X., Li, X., Wang, Z., Huang, Z., Huang, J., and Zhang, G. (2018). Tetrandrine enhances radiosensitivity through the CDC25C/CDK1/cyclin B1 pathway in nasopharyngeal carcinoma cells. Cell Cycle *17*, 671–680.

31. Fei, F., Qu, J., Liu, K., Li, C., Wang, X., Li, Y., and Zhang, S. (2019). The subcellular location of cyclin B1 and CDC25 associated with the formation of polyploid giant cancer cells and their clinicopathological significance. Lab. Invest. *99*, 483–498.

32. Wang, L., Xia, Y., Chen, T., Zeng, Y., Li, L., Hou, Y., Li, W., and Liu, Z. (2018). Sanyang Xuedai enhances the radiosensitivity of human non-small cell lung cancer cells via increasing iNOS/NO production. Biomed. Pharmacother. *102*, 618–625.

33. Itkonen, H.M., Urbanucci, A., Martin, S.E., Khan, A., Mathelier, A., Thiede, B., Walker, S., and Mills, I.G. (2019). High OGT activity is essential for MYC-driven proliferation of prostate cancer cells. Theranostics *9*, 2183–2197.

34. Monteiro, L.S., Diniz-Freitas, M., Warnakulasuriya, S., Garcia-Caballero, T., Forteza-Vila, J., and Fraga, M. (2018). Prognostic Significance of Cyclins A2, B1, D1, and E1 and *CCND1* Numerical Aberrations in Oral Squamous Cell Carcinomas. Anal. Cell. Pathol. (Amst.) *2018*, 7253510.

35. Wang, W., Shen, X.B., Jia, W., Huang, D.B., Wang, Y., and Pan, Y.Y. (2019). The p53/miR-193a/EGFR feedback loop function as a driving force for non-small cell lung carcinoma tumorigenesis. Ther. Adv. Med. Oncol. *11*, 1758835919850665.

36. Karsli Uzunbas, G., Ahmed, F., and Sammons, M.A. (2019). Control of p53-dependent transcription and enhancer activity by the p53 family member p63. J. Biol. Chem. *294*, 10720–10736.

37. Jin, S., Yang, X., Li, J., Yang, W., Ma, H., and Zhang, Z. (2019). p53-targeted lincRNA-p21 acts as a tumor suppressor by inhibiting JAK2/STAT3 signaling pathways in head and neck squamous cell carcinoma. Mol. Cancer *18*, 38.

38. Huang, C., Wu, S., Li, W., Herkilini, A., Miyagishi, M., Zhao, H., and Kasim, V. (2019). Zinc-finger protein p52-ZER6 accelerates colorectal cancer cell proliferation and tumour progression through promoting p53 ubiquitination. EBioMedicine *48*, 248–263.

39. Li, H., Zhang, Y., Dan, J., Zhou, R., Li, C., Li, R., Wu, X., Kumar Singh, S., Chang, J.T., Yang, J., and Luo, Y. (2019). p53 mutation regulates PKD genes and results in co-occurrence of PKD and tumorigenesis. Cancer Biol. Med. *16*, 79–102.

40. Fu, X., Wu, S., Li, B., Xu, Y., and Liu, J. (2020). Functions of p53 in pluripotent stem cells. Protein Cell *11*, 71–78.

41. Li, Y., Liu, X., Lin, X., Zhao, M., Xiao, Y., Liu, C., Liang, Z., Lin, Z., Yi, R., Tang, Z., et al. (2019). Chemical compound cinobufotalin potently induces FOXO1-stimulated cisplatin sensitivity by antagonizing its binding partner MYH9. Signal Transduct. Target. Ther. *4*, 48.